

See discussions, stats, and author profiles for this publication at: <https://www.researchgate.net/publication/337144991>

Hierarchical Action Encoding Within the Human Brain

Article in *Cerebral Cortex* · November 2019

DOI: 10.1093/cercor/bhz284

CITATIONS

0

READS

195

3 authors:



Luca Turella

Università degli Studi di Trento

42 PUBLICATIONS 702 CITATIONS

[SEE PROFILE](#)



Raffaella Ida Rumiati

Scuola Internazionale Superiore di Studi Avanzati di Trieste

212 PUBLICATIONS 4,341 CITATIONS

[SEE PROFILE](#)



Angelika Lingnau

Universität Regensburg

63 PUBLICATIONS 1,239 CITATIONS

[SEE PROFILE](#)

Some of the authors of this publication are also working on these related projects:



Food cognitive neuroscience [View project](#)



the neurochemical and neurocognitive basis of primary and social reward in humans [View project](#)

Hierarchical Action Encoding within the Human Brain

Luca Turella^{1}, Raffaella Rumiati², Angelika Lingnau^{1,3,4}*

1. Center for Mind/Brain Sciences - CIMEC, University of Trento, Italy
2. Scuola Internazionale Superiore di Studi Avanzati (SISSA), Italy
3. Department of Cognitive Sciences, University of Trento, Italy
4. Institute of Psychology, University of Regensburg, Germany

*** Correspondence:**

Dr. Luca Turella

Center for Mind/Brain Sciences - CIMEC, University of Trento

Via delle Regole, 101

38068, Trento (Italy)

luca.turella@gmail.com - luca.turella@unitn.it

Running title: Hierarchical Action Encoding

Key words: Action, fMRI, Grasping, Motor System, MVPA

Conflict of Interest. The authors declare no competing financial interests.

1 **Abstract**

2 Humans are able to interact with objects with extreme flexibility. To achieve this ability, the
3 brain does not only control specific muscular patterns, but it also needs to represent the abstract
4 goal of an action, irrespective of its implementation. It is debated, however, how abstract action
5 goals are implemented in the brain. To address this question, we used multivariate pattern analysis
6 of fMRI data.

7 Human participants performed grasping actions (precision grip, whole hand grip) with two
8 different wrist orientations (canonical, rotated), using either the left or right hand. This design
9 permitted to investigate a hierarchical organization consisting of three levels of abstraction: i)
10 *concrete action* encoding; ii) *effector-dependent goal* encoding (invariant to wrist orientation); and
11 iii) *effector-independent goal* encoding (invariant to effector and wrist orientation).

12 We found that motor cortices hosted joint encoding of concrete actions and of effector-dependent
13 goals, while the parietal lobe housed a convergence of all three representations, comprising action
14 goals within and across effectors. The left lateral occipito-temporal cortex showed effector-
15 independent goal encoding, but no convergence across the three levels of representation.

16 Our results support a hierarchical organization of action encoding, shedding light on the neural
17 substrates supporting the extraordinary flexibility of human hand behavior.

18 **Introduction**

19 Human behaviour is characterised by an astonishing dexterity combined with extreme flexibility.
20 How our motor system succeeds in implementing these two complementary features is still largely
21 unknown. Consider our daily goal-directed interactions within the environment, e.g. grasping an
22 object. On the one side, the brain coordinates the smooth execution of an articulated hand-object
23 interaction and its accurate online control. This is made possible through the representation of
24 *concrete* action exemplars characterised by specific *motor features*, such as the adopted type of
25 grip, effector and orientation of the hand with respect to the object. On the other side, to maintain
26 behaviour flexible, our brain also needs to represent the *abstract* goal of the action we aim to
27 perform, regardless of the concrete implementation of this action.

28 This example suggests that the neural architecture permitting our daily interactions with objects
29 represents action-related information at different levels of abstraction. The underlying idea is that
30 information characterizing an action, e.g. grasping different objects with specific grip types, might
31 be represented not only in the context of a specific movement (*concrete action level*), but also
32 generalizing across other motor features of the movement (*abstract goal levels*), such as the effector
33 and wrist orientation. We reasoned that brain regions jointly hosting concrete and abstract action
34 representations defined as above could subtend the neural basis which guarantees human hand
35 behaviour its incredible precision and extreme flexibility.

36 Neurophysiological and neuroimaging investigations demonstrated that a parieto-frontal motor
37 network is recruited during the planning, execution and online control of goal-directed hand actions
38 (Culham and Valyear 2006; Culham et al. 2006; Filimon 2010; Grafton 2010; Vesia and Crawford
39 2012; Turella and Lingnau 2014; Gallivan and Culham 2015; Janssen and Scherberger 2015; Fattori
40 et al. 2017). Recent findings hinted to the possibility that several regions within this network hosted
41 different levels of action encoding, ranging from the representation of a specific action to the
42 representation of the same action independently from other motor features.

43 A series of functional Magnetic Resonance Imaging (fMRI) studies adopting multivariate pattern
44 analysis (MVPA) investigated *concrete action representations*. For example, it has been
45 demonstrated that it is possible to distinguish between different actions performed with the
46 dominant hand, such as leftward vs rightward reaching or specific types of grasping performed
47 towards different objects or with different grip types (Gallivan, McLean, Valyear, et al. 2011;
48 Gallivan, McLean, Flanagan, et al. 2013; Fabbri et al. 2014) within the primary motor (M1),
49 premotor and posterior parietal cortices (PPC).

50 MVPA of fMRI (Gallivan, McLean, Smith, et al. 2011; Gallivan, McLean, Flanagan, et al. 2013;
51 Barany et al. 2014; Kadmon Harpaz et al. 2014; Krasovsky et al. 2014; Haar et al. 2015) and

52 Magnetoencephalography (MEG) data (Turella et al. 2016) has also been exploited to investigate a
53 more abstract level, namely, the generalization of an action across specific motor features, such as
54 the adopted effector (left vs right hand), the direction and/or the amplitude of the movement. These
55 abstract representations (also referred to as *action goals*) have been described within a
56 circumscribed set of cortical regions both at an *effector-dependent level* - representing actions
57 performed with the same effector (e.g. Kadmon Harpaz et al., 2014) - and an *effector-independent*
58 *level* - representing actions (or action goals) irrespective of the adopted effector (Gallivan, McLean,
59 Flanagan, et al. 2013).

60 Kadmon-Harpaz et al. (2014) showed that writing movements for specific letters performed with
61 the dominant hand were represented within a number of parietal and frontal regions (*concrete*
62 *action representation*). Of these regions, the M1 and aIPS in the left hemisphere also represented
63 the goal of the action, i.e. writing specific letters irrespective of the amplitude of the required
64 movement (*effector-dependent goal representation*). This finding suggests that two different levels
65 of action representations coexisted within M1 and aIPS.

66 Gallivan et al. (2013b) showed significant decoding for hand actions (grasping vs reaching)
67 during the planning phase of a movement within a wide set of motor, premotor and parietal areas. In
68 addition, several regions represented also the goal of the action (grasping vs. reaching) irrespective
69 of the adopted hand (*effector-independent goal representation*). Decoding for this type of
70 representation was obtained within bilateral regions of the posterior intraparietal sulcus (pIPS), and
71 the dorsal premotor cortex (PMd), middle (mIPS) and anterior intraparietal sulcus (aIPS) of the left
72 hemisphere.

73 Overall, the studies by Gallivan et al. (2013b) and Kadmon Harpaz et al. (2014) showed the joint
74 representation of concrete action instances and of abstract goal representation within several brain
75 regions including M1, premotor and parietal cortices. Together, the two studies suggest that there
76 might be a convergence of concrete, effector-dependent and effector-independent goal
77 representations within the parietal cortex in the left aIPS. However, since Gallivan et al. (2013b)
78 and Kadmon Harpaz et al. (2014) used qualitatively different types of hand actions, and since both
79 studies examined two different levels of representation, it is difficult to directly compare these
80 results. It thus remains unclear if more than two different levels of action representation are present
81 within the motor system and which, if any, brain regions jointly host these different types of action-
82 related information.

83 To address this question, we applied MVPA of fMRI data to examine which regions of the
84 human brain accommodate different levels of action encoding, ranging from the representation of
85 concrete action exemplars to the representation of their abstract goals. Participants were requested

86 to execute non-visually guided grasping actions (precision grip, whole hand grip) towards objects of
87 different sizes, performed with two different wrist orientations (canonical, rotated) and effectors
88 (left hand, right hand). Exploiting this experimental design in combination with MVPA, we aimed
89 to reveal a possible hierarchical structure of action representations including three different levels of
90 abstraction (see also Figure 2):

91 a) *concrete action encoding (level 1)*, representing different grasping actions performed with the
92 same effector and wrist orientation;

93 b) *effector-dependent goal encoding (level 2)*, representing different grasping actions performed
94 with the same effector but generalizing across wrist orientation;

95 c) *effector-independent goal encoding (level 3)*, representing different grasping actions
96 generalizing across both effector and wrist orientation.

97 The rationale of our experimental paradigm was three-folded: 1) to test whether visuo-motor
98 networks represented these different levels of action encoding following a hierarchical organization
99 along a concrete-to-abstract continuum, 2) to characterise cortical regions where these different
100 levels were jointly represented, and 3) to identify regions hosting all the three levels of action
101 encoding. Local processing within cortical sites hosting multiple levels of action representations
102 might permit to move between levels of the hierarchy, a fundamental neural computation for
103 supporting flexibility in our behaviour.

104 Based on previous neuroimaging and neurophysiological investigations (Culham and Valyear
105 2006; Culham et al. 2006; Filimon 2010; Grafton 2010; Vesia and Crawford 2012; Turella and
106 Lingnau 2014; Gallivan and Culham 2015; Janssen and Scherberger 2015; Fattori et al. 2017), we
107 predicted that actions are encoded at the concrete level of the hierarchy in a widespread set of
108 regions of the parieto-frontal hand motor network, consisting of motor, premotor and posterior
109 parietal cortices.

110 It is more difficult to predict which regions encode actions at the effector-independent and the
111 effector-independent goal level of the hierarchy since only few studies investigated these types of
112 representation (Gallivan, McLean, Flanagan, et al. 2013; Kadmon Harpaz et al. 2014). We expect
113 that these levels are represented within a subset of the regions hosting concrete action encoding,
114 with a possible central role of the intraparietal cortices.

115 Regarding the convergence of all three levels of action encoding, a likely candidate could be the
116 aIPS, as two independent fMRI studies suggested that this region might represent several different
117 levels within the hierarchy (Gallivan, McLean, Flanagan, et al. 2013; Kadmon Harpaz et al. 2014).

118 **Materials and Methods**

119 ***Participants***

120 24 participants took part in the experiment. Three participants were excluded from subsequent
121 analysis due to rapid head movements (exceeding 1 mm in translation or 1 degree of rotation within
122 one volume). The reported analyses refer to the remaining 21 participants (11 female, average age:
123 29.2 year, right-handed according to self-report). All participants gave written informed consent for
124 their participation in the study and were paid for their participation. The protocol of the study was
125 approved by the Ethics Committee for Human Research of the University of Trento in accordance
126 with the Declaration of Helsinki.

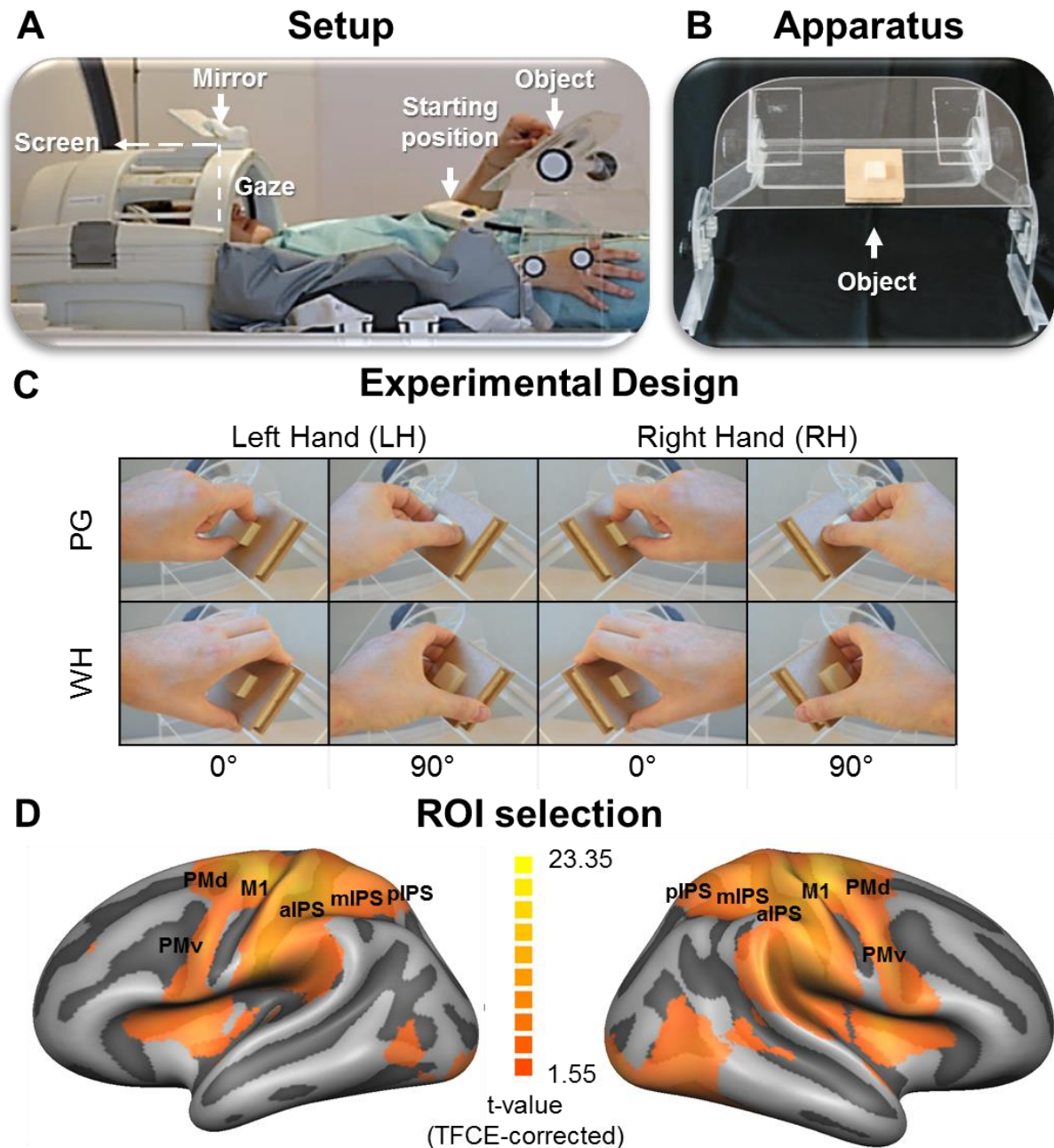
127

128 ***Experimental setup, task and paradigm***

129 The experimental setup was similar to the one described in a recent study on action planning
130 (Ariani et al., 2015). Participants were scanned while performing a motor task, which consisted in
131 executing non-visually guided grasping actions on an object (Figure 1A, B). The to-be-grasped
132 object was positioned on a Plexiglas MR-compatible support at the same reaching distance from
133 both hands (Figure 1A, B; see also Ariani et al., 2015). The object had a symmetrical shape and
134 comprised a flat surface with a small cuboid attached to it in a central position (Figure 1B). An MR-
135 compatible response box was adopted as the starting position (Figure 1A) permitting the recording
136 of reaction times (RTs). Participants were lying in the scanner horizontally, without tilting the head
137 towards the body (Figure 1A). Participants performed the movements without visual feedback of
138 the object or of their moving hand, following visual instructions projected on a screen behind the
139 head of the participant through a coil-mounted mirror. Visual stimulation was back-projected on the
140 screen (1024 x 768 resolution, 60 Hz refresh rate) using Presentation (version 16, Neurobehavioural
141 Systems, <https://www.neurobs.com/>). This setup prevented that any decoding results were affected
142 by the observation of the different actions during execution (see also Ariani et al. 2015, 2018 for
143 similar setups), at the cost of being less comparable to previous studies that used visually-guided
144 tasks.

145 We adopted a 2x2x2 factorial design (Figure 1C) with the factors: *wrist orientation* (no rotation,
146 0°, vs rotated wrist, 90°), *effector* (left hand, LH, vs right hand, RH), and *action* (precision grip, PG,
147 vs whole hand grip, WH). Participants were instructed to grasp two objects of different sizes.
148 Specifically, they were asked to perform a precision grip towards the small central block, using the
149 thumb and index finger (see Figure 1C, upper panel), and to perform a whole-hand grip using their

150 entire hand on the large lateral side of the object (see Figure 1C, lower panel). Participants had to
 151 perform the grasping action by simply touching the object, without manipulating or moving it. We
 152 adopted an object with a symmetrical shape, so that participants could grasp the object on their
 153 upper sides without any rotation of the wrist (0°), whereas the lateral sides could be grasped only by
 154 rotating the wrist (90°).



155
 156 **Figure 1. A. Experimental setup.** Participants were requested to perform non-visually guided grasping actions towards
 157 a wooden object. Visual instructions were projected on a screen behind the participant and could be seen via a mirror
 158 mounted on the head coil. The head of the participant was positioned in a conventional orientation, not tilted towards
 159 the object. The position of the head prevented the participant from seeing his own movement and the object during the
 160 entire experimental session. At the start of each trial, the hand rested on an MR-compatible response box. **B.**
 161 **Experimental apparatus.** The to-be-grasped object was attached on a Plexiglas support positioned above the pelvis of
 162 the participant. The wooden object consisted of two elements, a small cuboid (2x2x1 cm) attached over a larger one
 163 (7x7x2 cm). **C. Experimental design.** We used a 2x2 factorial design with factors: *wrist orientation* (canonical, 0° ;

164 rotated, 90°), *effector* (right hand, RH; left hand, LH), and *action* (precision grip, PG, whole hand, WH). **D. ROI**
165 **selection.** The position of the ROIs selected for MVPA are reported on the brain surface (see Supplementary Materials,
166 Figure S2, for axial and coronal views and three-dimensional render of the ROI positions). We superimposed the
167 statistical t-maps assessing the univariate contrast [grasping > baseline] on the reconstructed brain surface. The
168 minimum threshold for the t-map was set at $p < 0.05$ TFCE corrected (two-tailed, $z = 1.96$).

169

170 Each participant completed one experimental session consisting of 10 runs (Figure S1). Each run
171 consisted of 64 experimental trials arranged in 8 blocks (Figure S1). Within each run, the effector to
172 perform the action (left or right hand) was constant. The order of the hand to be used was alternated
173 across runs and counterbalanced across participants. Each run started with an initial baseline period
174 (20 s), followed by four blocks of trials (each lasting 28 s), interleaved with a baseline period (8 s),
175 a long baseline period (32 s), four blocks of trials (each lasting 28 s) interleaved with a baseline
176 period (8 s) and a final baseline period (24 s; see Figure S1).

177 Visual stimulation during the baseline period consisted of a grey fixation cross on a black
178 background. At the beginning of each block, we presented an instruction (3 s) signalling the
179 orientation of the hand for the following block. The instruction consisted of a vertical line,
180 signalling the participant to use an untilted wrist (canonical, 0°), grasping the upper side of the
181 object, or in a horizontal line, indicating to use a tilted wrist (rotated, 90°), grasping the lateral side
182 of the object. The instruction was followed by the presentation of a black fixation cross (1 s),
183 followed by a block of eight experimental trials. Each experimental trial lasted 2.5 s and was
184 followed by a black fixation cross (0.5 s). Each experimental trial consisted of a change in the color
185 of the fixation cross which instructed the participant which action to perform. We adopted four
186 different colors for the cue (blue, green, red, yellow). For each participant, each color was
187 associated with the execution of an action (either PG or WH) with a specific effector (either left or
188 right hand). The colors assigned to each combination of action and effector were counterbalanced
189 across participants. At the appearance of the cue, the participant had to perform the action and then
190 return to the starting position waiting for the next cue.

191 To avoid that participants might establish the same arbitrary mapping between an action and a
192 color across the two hands, we adopted different colors for signaling the same actions across the
193 two hands. Therefore, cross-decoding at the most abstract level cannot be based on arbitrary
194 stimulus response mappings unless one assumes that the same patterns of brain activation are
195 elicited for all four combinations between color and action.

196 We recorded the participants' behavioural performance using a video camera mounted on a
197 tripod outside the 0.5 mT line during the entire duration of the study for offline control of
198 behaviour. To familiarize with the task, participants practised two entire runs (one for each hand)
199 before entering the MR room and one additional practise run inside the MR scanner.

200 ***Data Acquisition***

201 MR data were acquired with a 4T scanner (Bruker MedSpec) using an 8-channel head coil.
202 Functional images were acquired with a T2* echo-planar imaging (EPI) sequence (TR 2 s; TE 33
203 ms; FOV: 192 × 192 mm; in-plane resolution 3x3; 28 slices with slice thickness of 3 mm and a gap
204 size of 0.45 mm acquired in ascending interleaved order and aligned parallel with the ACPC line).
205 Before each run, an additional scan was collected to measure the point-spread function of the
206 acquired sequence to correct possible distortions (Zaitsev et al. 2004). Each participant completed
207 10 runs of 174 volumes each. At the beginning of the experimental session, a T1-weighted MP-
208 RAGE anatomical scan (TR: 2700 ms; TE: 4.18 ms; FOV: 256 x 224 mm; 1 mm isotropic voxel
209 resolution; 176 slices) was acquired for each participant.

210

211 **Experimental Design and Statistical Analysis**

212 ***Behavioural analysis***

213 For behavioural analysis and MVPA, we excluded trials based on performance errors off-line by
214 visual inspection of the videos recorded during the experiment (e.g. when participants performed
215 the incorrect grasping action, the right grip with the wrong wrist orientation or when they omitted to
216 perform the action). Moreover, we excluded trials if the RT was shorter than 100 ms or longer than
217 1500 ms (for a similar procedure, see Ariani et al., 2015). On average, we excluded 13 out of a total
218 of 640 trials (~2 %), indicating that participants were able to perform the task correctly. A 2x2x2
219 repeated measure ANOVA was performed on the RTs.

220

221 ***fMRI data pre-processing and analysis***

222 Data analysis was performed using BrainVoyager QX 2.8.4 (Brain Innovation), custom software
223 written in MATLAB (MathWorks), the Neuroelf Toolbox (<http://neuroelf.net/>) and the
224 CoSMoMVPA Toolbox (Oosterhof et al., 2016, <http://www.cosmomvpa.org/>). We excluded the
225 first four functional volumes from analysis to avoid possible T1 saturation effects. Pre-processing
226 started with the realignment of all functional images with the first image of the first run as reference
227 using trilinear interpolation. Subsequently, we applied slice time correction and high-pass filtering
228 (cut-off frequency of 3 cycles per run). Next, we co-registered the first volume of the first run to the
229 T1 anatomical image. For group analysis, anatomical and functional data were transformed into

230 Talairach space using trilinear interpolation. For univariate analysis, functional images were
231 smoothed with a Gaussian kernel of 8-mm full width half maximum. No spatial smoothing was
232 applied for multivariate analysis.

233

234 *Univariate analysis*

235 For ROI selection, we defined a General Linear Model (GLM) for each participant, with a total
236 of three predictors of interest, corresponding to the two different types of movements (precision
237 grip, whole hand grasp), performed either with the left or right hand, and the instructions (see
238 Figure S1). The predictors were created with a boxcar convolved with hemodynamic response
239 function (Boynton et al., 1996). For the instructions, the start and end of the boxcar function was
240 defined by their onset and offset (duration: 3 seconds). For the left and right hand conditions, we
241 selected a box-car starting at the onset of the first experimental trial of each block and with a
242 duration of 24 seconds, so that it comprised the 8 experimental trials. This model was selected to
243 maximize the power of the design to identify the cortical regions recruited by the task.

244 The estimated beta weight for each condition was transformed to percent signal change and
245 random effect analysis (RFX) was conducted at the group level. Statistical analysis (one-sample t-
246 test) was performed using the CoSMoMVPA Toolbox (Oosterhof et al. 2016,
247 <http://www.cosmomvpa.org/>). Correction for multiple comparisons was performed using
248 Threshold-Free Cluster Enhancement (TFCE, Smith and Nichols, 2009) in combination with cluster
249 level correction ($p < 0.05$, two-tailed, $z > 1.96$, 10,000 permutations) as implemented in
250 CoSMoMVPA. Statistical maps (t-values masked with TFCE threshold) were projected onto an
251 average surface map of the reconstructions of the cortical surface of the left and right hemisphere of
252 all participants that were included in this study, using cortex-based alignment as implemented in
253 Brain Voyager (version 2.8).

254

255 *ROI selection for MVPA*

256 We aimed to identify cortical regions representing different levels of action encoding, and
257 cortical regions in which the different levels are jointly represented. We reasoned that the
258 identification of regions showing overlapping representations might support the possible exchange
259 of information across different levels of the hierarchy within these cortical sites.

260 To this aim, we selected ROIs within both hemispheres based on previous studies that examined
 261 the encoding of movement goals at different levels of abstraction (Gallivan, McLean, Flanagan, et
 262 al. 2013; Kadmon Harpaz et al. 2014). We decided to start from the results of a recent study
 263 (Gallivan, McLean, Flanagan, et al. 2013) that adopted hand movements (grasping and reaching
 264 actions) similar to the ones considered in our study. Moreover, this study investigated two levels of
 265 action encoding, *concrete action* and *effector-independent goal* representations, allowing us to
 266 replicate and extend their findings investigating an additional intermediate level of representation.
 267 For each ROI, we started from the activation at the group level obtained in Gallivan et al. (2013).
 268 Then, we located the nearest local maxima within the results of the univariate GLM RFX analysis
 269 (t-contrast: left and right hand vs. baseline). We focused on the following ROIs: M1, ventral
 270 premotor cortex (PMv), dorsal premotor cortex (PMd) and regions along the intraparietal sulcus,
 271 pIPS, mIPS and aIPS (anterior aIPS in Gallivan et al. 2013). The positions of the peaks for each
 272 group ROI are reported in Table 1, illustrated in Figure 1D and reported in more detail in Figure S2.

Coordinates (Talairach)

ROI	x	y	z
Left pIPS	-21	-70	48
Right pIPS	20	-62	45
Left mIPS	-31	-53	48
Right mIPS	30	-50	51
Left aIPS	-40	-32	46
Right aIPS	37	-29	48
Left M1	-31	-24	54
Right M1	31	-25	51
Left PMd	-22	-11	48
Right PMd	26	-13	52
Left PMv	-53	-4	40
Right PMv	54	1	35

273 **Table 1. Position of the ROIs used for MVPA.**

274

275 ***ROI-based and searchlight-based MVPA***

276 For MVPA, we estimated a GLM for each participant. We modeled each trial (see Figure S1) as
 277 a boxcar function convolved with the hemodynamic response function (Boynton et al., 1996). The
 278 onset and duration of the boxcar was based on the presentation of the visual cue, with a duration of
 279 2 seconds.

280 We considered two regressors for each block (Figure S1), modelling all trials for each
281 experimental condition within a block as a single predictor of interest (for a similar procedure see
282 Oosterhof et al., 2012a, 2012b). For each participant, a total of 160 regressors of interest were
283 considered, originating from the 8 (2 movement types x 2 wrist orientations x 2 effectors)
284 conditions x 5 runs (for each hand) x 4 blocks. In addition, we considered instructions, movement
285 parameters (3 for translation, 3 for rotation) and error trials, if present, as predictors of no interest.
286 For the instructions, their onset and offset (duration: 3 s) was used as the start and end of the boxcar
287 function.

288 For classification, we used Linear Discriminant Analysis (LDA) as implemented in the
289 CoSMoMVPA Toolbox (Oosterhof et al., 2016). MVPA was performed adopting a ROI-based and
290 a volume-based searchlight approach (Kriegeskorte and Bandettini 2007), i.e. performing a
291 decoding analysis along all the voxels within the brain. The searchlight analysis was conducted to
292 provide a replication and a possible extension of the results of the ROI analysis. Note that the
293 dimensions of the searchlight limit the spatial specificity of the results. This is a limitation inherent
294 to any MVPA as the result of decoding analysis for each searchlight is assigned to the central voxel
295 of the searchlight (Oosterhof et al. 2011). Each ROI and each searchlight were defined using the
296 beta values of the selected voxel and of the surrounding neighbouring ones within a sphere with a
297 radius of four voxels (average of 218.6 voxels per searchlight and of 250.2 voxels for ROIs).
298 The estimated beta weights for each predictor of interest were adopted as features for the classifier.
299 We extracted 20 patterns of beta weights for each condition.

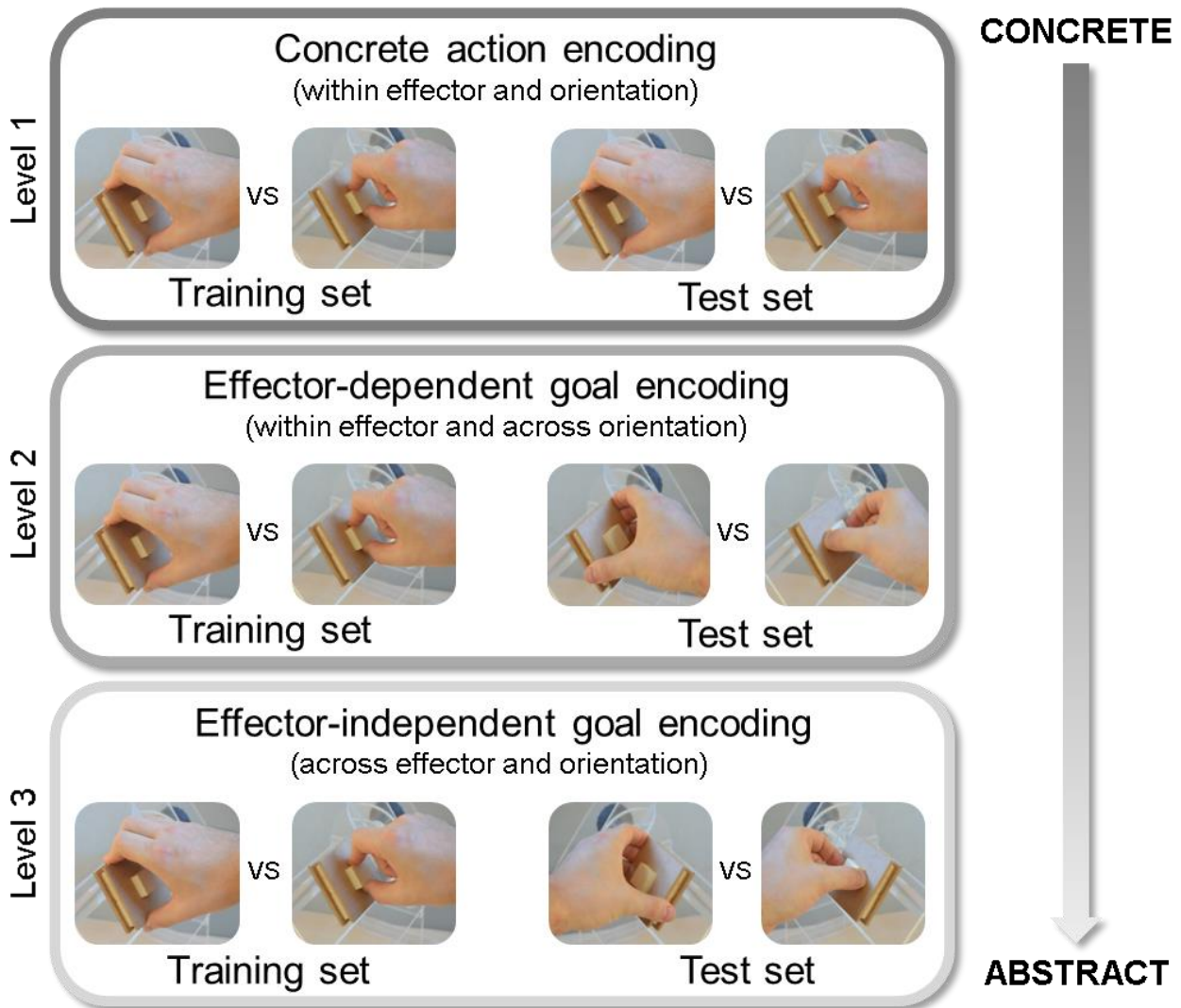
300 Our analysis investigated the possible hierarchical organization of action encoding along a
301 concrete-to-abstract continuum (see Figure 2), focusing on three levels of representation:

302 Level 1: *concrete action encoding*;

303 Level 2: *effector-dependent goal encoding*, generalizing across wrist orientation;

304 Level 3: *effector-independent goal encoding*, generalizing across effector and wrist orientation.

Hierarchical action encoding



305 **Figure 2. A. Hierarchical action encoding and decoding approach.** Schematic overview of the hierarchical
306 organization of action encoding tested within this study, consisting of three levels of representation along a concrete-to-
307 abstract continuum. An example of the type of adopted decoding procedure is provided within the inset for each level of
308 action representation.

309

310 In analogy with previous studies (Gallivan, McLean, Smith, et al. 2011; Gallivan, McLean,
311 Flanagan, et al. 2013; Gallivan, McLean, Valyear, et al. 2013; Tucciarelli et al. 2015; Turella et al.
312 2016), we adopted cross-decoding for testing abstract goal encoding, i.e. generalizing across
313 specific motor features, by training the classifier on a pairwise comparison having a specific motor
314 feature and testing it on a different pairwise comparison lacking this feature.

315 To estimate decoding accuracy, we adopted a leave-one-run-out cross-validation approach. We
316 adopted a nested approach for decoding following Barany et al. (2014) whereby the same data were

317 used for training the classifier within each searchlight, making the results across the different levels
318 of action encoding comparable. Within each cross-validation fold, for all the considered pairwise
319 comparisons, we tried to distinguish between the two action types (PG vs. WH) by training the
320 classifier on the beta patterns extracted from four runs (16 per condition) and testing it on the
321 patterns estimated from another run with independent data (4 per condition).

322 To test for the encoding of *concrete actions* (level 1; Figure 2, upper panel), we considered
323 grasping movements performed with a specific effector and wrist orientation, training and testing
324 the classifier on independent data of the same pairwise comparison (e.g., training and testing: WH
325 0° RH vs. WH 0° RH). All possible combinations of training and testing sets were considered,
326 separately for each hand.

327 For *effector-dependent goal encoding* (level 2; see Figure 2, middle panel), we trained the
328 classifier on the pairwise comparison on one hand (e.g., training: WH 0° RH vs PG 0° RH) and then
329 tested the classifier on the same pairwise comparison, but with a different wrist orientation (e.g.,
330 testing: WH 90° RH vs PG 90° RH). This type of encoding was tested for each effector separately
331 with all possible combinations of training and testing sets.

332 For *effector-independent goal encoding* (level 3; see Figure 2, bottom panel), we trained a
333 classifier on a specific pairwise comparison between the two actions (e.g., training: WH 0° RH vs
334 PG 0° RH) and then tested it on the same pairwise comparison but performed with the other effector
335 and wrist orientation (e.g., testing: WH 90° LH vs PG 90° LH). For this level, decoding results for
336 all possible combinations of training and testing sets with the two different effectors were
337 considered.

338 For ROI-based MVPA, we tested significant decoding with a one-sample t-test against chance
339 level (50%). We report uncorrected and corrected results adopting False Discovery Rate (FDR)
340 correction (Benjamini and Hochberg 1995) accounting for multiple comparisons considering all
341 comparisons ($N = 5$) within all ROIs ($N = 12$).

342 For the searchlight MVPA, to determine in which brain areas decoding was above chance level
343 (50 %, Oosterhof et al. 2016), we computed t-tests across the individual decoding accuracy maps. P
344 values were set at $p < 0.05$ (one-tailed, $z > 1.6449$) for cluster level correction adopting TFCE
345 (Smith and Nichols 2009) estimated adopting 10,000 permutations as implemented in
346 CoSMoMVPA.

347 To further characterize the z maps obtained from the searchlight MVPA, we entered them into a
348 conjunction analysis. The conjunction was set at the voxel level by considering the minimum z
349 value across the considered maps (Nichols et al. 2005). Statistical maps originating from searchlight
350 analyses were projected onto an average surface map computed using cortex-based alignment (as
351 implemented in BrainVoyager 2.8) of the anatomies of all participants that were included in this
352 study.

353

354 **Results**

355 *Behavioural results*

356 The 2x2x2 repeated measures ANOVA performed on RTs showed no significant main effect nor
357 an interaction (effector: [$F_{(1,20)} = 0.57, p = 0.46$]; action [$F_{(1,20)} = 3.20, p = 0.09$]; orientation [$F_{(1,20)}$
358 $= 3.19, p = 0.09$]; effector x action [$F_{(1,20)} = 0.65, p = 0.8$], effector x orientation [$F_{(1,20)} = 0.52, p =$
359 0.48]; orientation x action [$F_{(1,20)} = 1.92, p = 0.18$]; effector x action x orientation [$F_{(1,20)} = 0.42, p =$
360 0.53]). Mean RTs are plotted and reported in the supplementary materials (Figure S2 and Table S1).

361

362 *Univariate results*

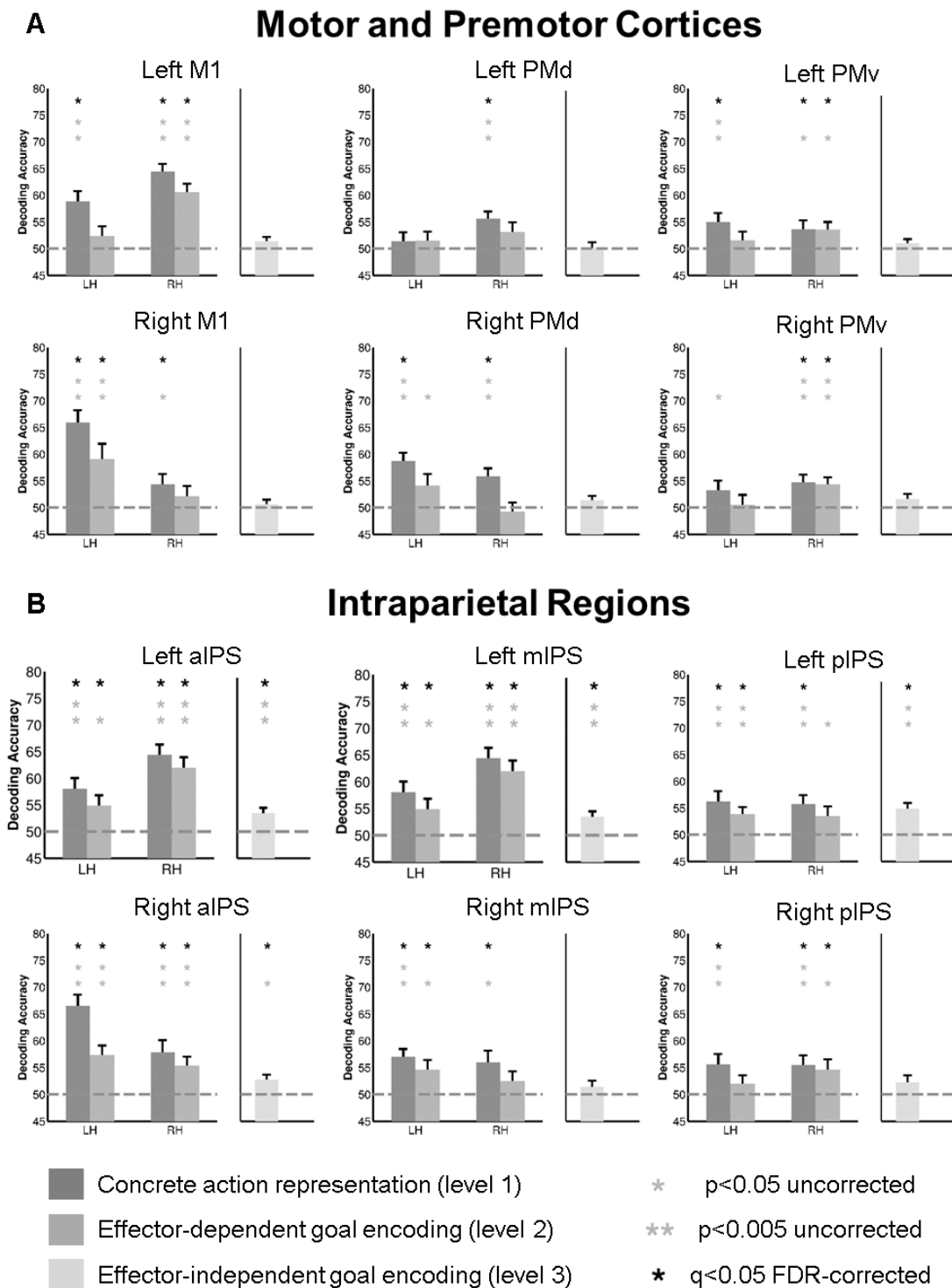
363 Univariate analysis was adopted to identify brain regions involved in non-visually guided
364 grasping execution adopting the left and the right hand. The contrast of interest identified cortical
365 regions recruited during the task, i.e. grasping conditions (left and right hand) vs baseline. This
366 contrast revealed the recruitment of a widespread bilateral set of regions within the premotor cortex,
367 M1, somatosensory cortex and PPC (Figure 1D). In addition, we observed a bilateral recruitment of
368 the posterior temporal cortex, the parietal operculum and the insular cortex.

369

370 *ROI-based MVPA*

371 Our results showed significant decoding of grasping actions for all three investigated levels of
372 representation, suggesting a hierarchical organization of action encoding across frontal and
373 intraparietal cortices (see Figure 3A, B). We started focusing on the three levels to provide a general
374 overview of the structure of action organization within the parieto-frontal motor network. Then, to

375 better characterise which brain regions host overlapping action representations, we provided a
 376 description of the joint encoding of these different levels, separately for frontal and parietal regions.



377

378 **Figure 3. A. Decoding results for ROI-based MVPA: motor and premotor cortices. B. Decoding results for ROI-**
 379 **based MVPA: intraparietal regions.** The bar graphs show the average decoding accuracy for the different levels of
 380 action encoding. Significant decoding is indicated with asterisks (p<0.05, *, p<0.005, **; q<0.05 FDR corrected, black
 381 star).

382

383 *Representation of different levels of action encoding*

384 The results of the ROI-based MVPA revealed that actions are encoded at the concrete level
385 (level 1 in Figure 2), characterized by a specific combination of hand orientation and adopted
386 effector, in a widespread set of regions. All ROIs encoded specific grasping actions performed with
387 the contralateral hand (Figure 3A, B).

388 These findings are in line with the role of parieto-frontal motor networks in effector-specific
389 action planning for saccade and hand movements (Rizzolatti et al. 1998, 2014; Cui and Andersen
390 2007; Andersen et al. 2014). With respect to hand actions, our description mirrors the general
391 selectivity for this type of actions present both in PPC, premotor and motor cortices (Turella and
392 Lingnau 2014; Gallivan and Culham 2015; Janssen and Scherberger 2015; Fattori et al. 2017).
393 Moreover, our results are well in agreement with previous MVPA studies in humans (Gallivan,
394 McLean, Valyear, et al. 2011, 2013; Gallivan, McLean, Flanagan, et al. 2013; Fabbri et al. 2014)
395 and monkey studies (Nelissen et al. 2017) examining similar grasping conditions.

396 Within most of our ROIs, we also obtained a representation of concrete ipsilateral hand actions
397 (level 1, Figure 3). This is in agreement with the predominant representation of contralateral hand
398 actions described in neurophysiological (Chang et al. 2008; Chang and Snyder 2012),
399 neuropsychological (Karnath and Perenin 2005; Andersen et al. 2014) and neuroimaging studies
400 (Valyear and Frey 2015). Even if the representation of ipsilateral hand movements has been
401 investigated less intensely, our findings are in line with human fMRI investigations (Beurze et al.
402 2007; Gallivan, McLean, Flanagan, et al. 2013; Valyear and Frey 2015; Fitzpatrick et al. 2019) and
403 monkey neurophysiological studies (Rizzolatti et al. 1988; Chang et al. 2008; Michaels and
404 Scherberger 2018).

405 It is more difficult to relate our results for the abstract representations (level 2, level 3) to
406 previous investigations as only few studies (Gallivan, McLean, Flanagan, et al. 2013; Kadmon
407 Harpaz et al. 2014) investigated similar action representations while adopting different experimental
408 paradigms.

409 Significant decoding for the second level (*effector-dependent goal encoding*) was evident in a
410 less extended set of regions (Figure 3A, B). In general, there was a posterior-to-anterior gradient
411 with a higher number of regions with significant decoding for this level of representation within
412 PPC with respect to frontal cortex. Several PPC regions showed significant decoding for the second
413 level jointly for the ipsi- and contralateral hand, whereas no frontal region showed this pattern of
414 results.

415 Finally, none of the frontal regions accommodated all three investigated levels of action
416 encoding (Figure 3A), whereas there was significant decoding for the third level (*effector-*
417 *independent goal encoding*) within several regions of PPC (bilateral aIPS, left pIPS).

418 *Convergence of action representations within frontal cortices*

419 The ROI-based analysis showed a similar pattern of decoding for left and right M1 (Figure 3A).
420 There was a joint representation of concrete action and effector-dependent goal representation for
421 the contralateral hand (levels 1 and 2). In addition, there was a representation of concrete actions
422 performed with the ipsilateral hand (level 1), but no effector-dependent goal representation (level
423 2).

424 Premotor cortices led to more variable results (Figure 3A). Left PMd presented significant
425 decoding only for concrete actions performed with the contralateral hand (RH). Right PMd showed
426 a pattern of decoding similar to right M1 (significant decoding of level 1 and 2 for LH, significant
427 decoding of level 1 for RH). Left and right PMv showed a pattern of decoding similar to left M1
428 (significant decoding of level 1 and 2 for RH, significant decoding of level 1 for LH). The
429 difference in decoding within premotor regions might be in part related to differences in action
430 representations for the dominant and non-dominant hand.

431 Taken together, our results suggest that frontal regions might be involved in representing
432 concrete, specific ipsilateral and contralateral action exemplars, together with the goal of
433 contralateral hand actions at an intermediate - effector-dependent - level of abstraction. This
434 organization of action representations might allow the conversion of a goal into a specific action but
435 only at the effector-dependent level, e.g. changing hand position on the grasped object, using the
436 same hand. This suggests a possible role of motor and premotor cortices as a neural substrate
437 subtending flexible hand behaviour but limited to the contralateral effector.

438

439 *Convergence of action representations within parietal regions*

440 For intraparietal regions, MVPA revealed a qualitatively different picture (Figure 3B). First,
441 there was a more widespread representation of concrete action (level 1) and effector-dependent goal
442 encoding (level 2) for the ipsilateral and contralateral hand. Importantly, several regions showed

443 significant effector-independent encoding (level 3). In contrast to frontal cortices, there were several
444 regions hosting all three levels of action encoding (Figure 3B), namely, bilateral aIPS and left pIPS.

445 The description of effector-independent goal representations within the PPC is in line with the
446 two MVPA studies which inspired our investigation (Gallivan, McLean, Flanagan, et al. 2013;
447 Kadmon Harpaz et al. 2014). In particular, our results are comparable to those of Gallivan et al
448 (2013) which showed goal representations within similar regions of the PPC (aIPS) adopting similar
449 MVPA methods.

450 Note that our results are partially different from a recent repetition suppression fMRI study
451 (Valyear and Frey 2015). In this study, Valyear & Frey (2015) did not obtain any evidence for
452 grasp-specific hand-independent representations as we did in our study. The authors mainly
453 described hand-specific representations within the PPC. The difference between the two studies
454 might be related to the adopted methods – different sensitivity of repetition suppression and
455 MVPA- and/or the adopted experimental design, as our non-visually-guided task might engage a
456 specific set of action representations. That said, the two results are not mutually exclusive as there
457 might be a strong effector-specific gradient within the PPC as shown by Valyear and Frey (2015) -
458 and by a long tradition of neurophysiological, neuropsychological and neuroimaging studies
459 (Andersen et al. 2014), whereas there might also exist an effector-independent functional gradient
460 within the PPC as suggested by recent studies (Heed et al. 2011; Leoné et al. 2014).

461 Overall, our results suggest that intraparietal regions (aIPS, left pIPS) host overlapping
462 representations of concrete exemplars of actions and goals at an intermediate level - effector-
463 dependent – for both hands, but also at a more general effector-independent level. Within these
464 cortical sites, this organization might allow sharing of information across all three levels. Brain
465 regions having this property could allow local computations across different levels of the hierarchy
466 allowing the flexible remapping of goals across effectors and means, e.g. changing the hand
467 adopted to grasp the same object with a different wrist orientation.

468

469 ***MVPA Searchlight***

470 *Level 1: concrete action encoding (within effector and orientation)*

471 Significant decoding for concrete actions (level 1, see Figure 2, upper panel) was evident within
472 a widespread set of frontal, parietal and temporal areas for each hand separately (Figure S4, S5).

473 These regions encoded concrete effector-dependent actions, i.e. specific exemplars defined by a
474 combination of wrist orientation and action type.

475 Our results for the right hand are well in agreement with then known with previous human and
476 monkey studies (Fattori et al. 2010, 2017; Vesia and Crawford 2012; Turella and Lingnau 2014;
477 Gallivan and Culham 2015; Janssen and Scherberger 2015; Breveglieri et al. 2016), and with
478 previous MVPA neuroimaging investigations (Gallivan, McLean, Valyear, et al. 2011, 2013;
479 Gallivan, McLean, Flanagan, et al. 2013; Fabbri et al. 2014; Ariani et al. 2015). As for the left hand,
480 there are few neurophysiological and neuroimaging investigations on action representations
481 performed with this effector (for exceptions, see Fabbri et al., 2010; Gallivan et al., 2013a, 2013b;
482 Valyear and Frey, 2015), so it is difficult to make direct comparisons. Qualitatively, however,
483 results for the two hands seem comparable and specular with maximum decoding within the
484 contralateral M1.

485

486 *Level 2: effector-dependent goal encoding (within effector and across orientation)*

487 The intermediate level of action encoding (level 2, see Figure 2, middle panel) was identified
488 through MVPA cross-decoding as an effector-dependent goal representation, generalizing across
489 wrist orientation. We identified this type of encoding for the two effectors separately (Figure S6,
490 S7).

491 For the left hand (Figure S6), there was a lateralization of significant decoding in the frontal
492 cortex, mainly within the contralateral (right) M1, somatosensory and premotor cortices. Moreover,
493 there was bilateral significant decoding within the superior and inferior parietal cortex. Within the
494 temporal lobe, there was also significant decoding within the posterior lateral occipitotemporal
495 cortex (LOTC) of the right hemisphere.

496 For the right hand (Figure S7), a specular and more widespread pattern of results was evident
497 within the frontal cortex with significant decoding within the left M1, premotor and somatosensory
498 cortices (Figure S7). Bilateral significant decoding was evident within the superior and inferior
499 parietal lobule encompassing the intraparietal sulcus. For the temporal lobe, the bilateral posterior
500 part of the LOTC was showing significant decoding.

501

502 *Regions of convergence for concrete action and effector-dependent goal encoding (conjunction of*
503 *levels 1 and 2)*

504 To identify cortical sites with a convergence of concrete action and effector-dependent goal
505 encoding (levels 1 and 2), we performed a conjunction analysis, separately for each hand (Figure
506 S8, S9). The threshold value for the conjunction maps needs to be interpreted as if the two corrected
507 maps are independently significant at the given p-value. The minimum level of significance ($z=$
508 1.6449 , $p=0.05$) is equivalent to a real p value of $=0.05^2$, i.e. $p = 0.0025$.

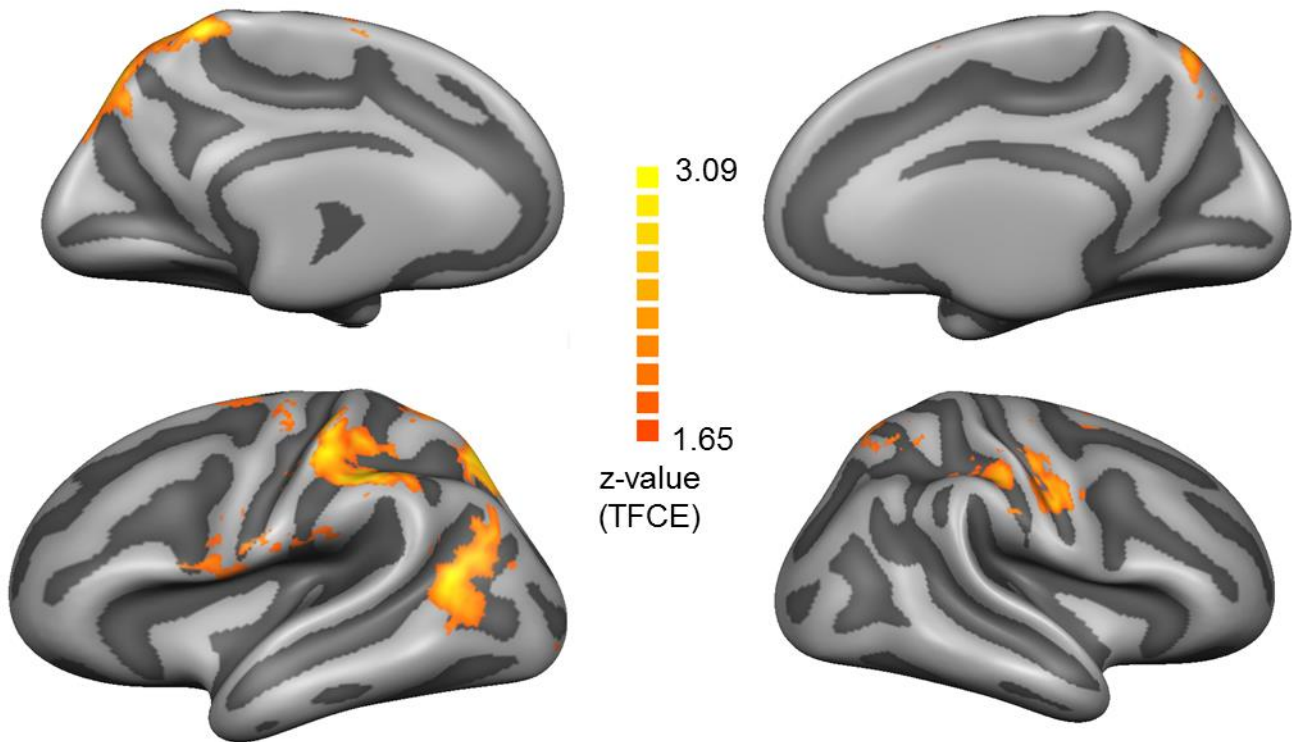
509 For both effectors, there was a clear lateralization of the conjunction of these representations
510 within a cluster comprising the contralateral premotor, motor, somatosensory and posterior parietal
511 cortices (see Figure S8, S9). The results of the searchlight analyses thus confirmed the ROI-based
512 MVPA, which showed a lateralization of the joint representation of level 1 and 2 for each hand only
513 within the contralateral motor cortices (Figure 3A). Moreover, we obtained a convergence of levels
514 1 and 2 within bilateral posterior parietal and mainly within the right posterior temporal cortex for
515 both effectors (Figure S8, S9).

516

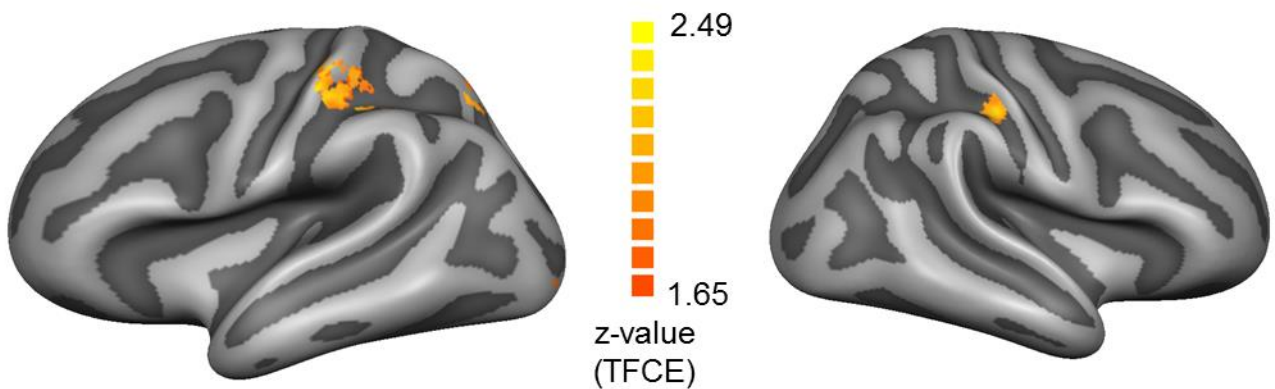
517 *Level 3: Effector-independent goal encoding (across effector and orientation)*

518 The most abstract level of encoding (level 3, see Figure 2, bottom panel) was identified through
519 MVPA cross-decoding as a goal representation, generalizing across the adopted effector and wrist
520 orientation (Figure 4A). Within frontal cortex, significant cross-decoding was evident within the
521 right PMv, the left PMv and PMd. Furthermore, two clusters showed significant decoding within
522 bilateral posterior parietal cortices, within the aIPS and posterior superior parietal lobule (pSPL)
523 spreading within the posterior part of the intraparietal sulcus (pIPS). Within the lateral occipito-
524 temporal cortex, a significant cluster was present within the left anterior part of the posterior middle
525 temporal gyrus (pMTG). Our results are partially in agreement with two recent investigations
526 adopting similar cross-effector decoding (Gallivan, Chapman, et al. 2013; Gallivan, McLean,
527 Flanagan, et al. 2013; Turella et al. 2016).

A Effector-independent goal encoding



B Conjunction of all action representations



528 **Figure 4. A. Effector-independent goal encoding.** A z-map assessing the statistical significance of the decoding
529 accuracies is represented. The threshold was set at $p < 0.05$ TFCE corrected (one-tailed). Upper panel: medial view of
530 the brain. Lower panel: lateral view of the brain. **B. Conjunction analysis for all action representations.** The
531 statistical map represents the minimum z values for the conjunction of the five statistical maps (one map for each
532 effector for levels 1 and 2, and one map for level 3). The threshold was set at $p < 0.05$ TFCE corrected (one-tailed, $z =$
533 1.6449).

534 *Regions of convergence for all action and goal representations (conjunction of levels 1, 2 and 3)*

535 To identify additional brain areas in which all three investigated action levels are jointly
536 represented, and that we might have missed in the ROI analysis, we performed a conjunction
537 analysis on the searchlight maps for all three levels of action representations (*concrete*, level 1,
538 *effector-dependent*, level 2, and *effector-independent*, level 3). To this aim, we performed a
539 conjunction analysis of five z-maps: one map for each effector of level 1 (Figure S4, S5); one map
540 for each effector of level 2 (Figure S6, S7), and one map for level 3 (Figure 4A). The threshold
541 value for the conjunction map needs to be interpreted as if the five corrected maps are all
542 independently significant at the given p-value. The minimum level of significance ($z= 1.6449$,
543 $p=0.05$) is equivalent to a real p value of $=0.05^5$, i.e. $p = 0.0000003125$.

544 A significant conjunction was evident within three sites in the posterior parietal cortex (Figure
545 4B). The first two sites were obtained within the bilateral aIPS. The other cluster was located within
546 the superior parietal lobule (pSPL) spreading within the posterior part of the intraparietal sulcus
547 (pIPS). A left lateralization of effector-independent action encoding was evident also in results by
548 Gallivan et al (2013). Our analysis led to no significant clusters within the frontal lobe and thus
549 confirmed the results of the ROI analysis.

550 Overall, ROI-based MVPA and searchlight analyses suggested a differential role for frontal,
551 parietal and temporal regions, revealing a complex hierarchical structure of action representations
552 hosted within the human brain.

553 **Discussion**

554 In this study, we aimed to identify brain areas that represent actions at three increasing levels of
555 abstraction, and areas that jointly accommodate all three levels. We found a different pattern of
556 functional specificity for frontal, parietal, and temporal cortices. Moreover, we identified a
557 convergence of all three levels in parietal cortex.

558 These results support the idea of a complex hierarchical structure of these representations hosted
559 within the human brain which might be at the basis of the extreme flexibility of our daily behaviour,
560 remapping an intended motor goal (through the same effector, e.g. by using a different wrist
561 orientation), or even generating a different motor output (adopting another effector).

562 Within the *frontal lobe*, ROI analysis revealed a convergence of concrete action and effector-
563 dependent goal representations (levels 1 and 2) for the contralateral hand within primary motor
564 cortices (see also Figure S8, S9). M1 might provide the neural substrate for representing a very
565 specific action together with abstract information about its goal, but only at an effector-dependent
566 level.

567 Within the *parietal lobe*, we obtained a convergence of all three action representations (levels 1,
568 2 and 3), ranging from the representation of hand-specific action exemplars to the representation of
569 effector-independent goals. The joint coding of all three different representations in bilateral aIPS
570 and left pIPS suggests a role of these regions as a central hub for moving across representations
571 along the hierarchy, from concrete action specification to goals within and across different
572 effectors.

573 Within the left *lateral occipito-temporal lobe*, searchlight analysis showed a more segregated
574 organization, with the left LOTC hosting wrist- and effector-independent action representations, but
575 no convergence with concrete and effector-dependent action encoding (see Figure 4A, B).

576 We acknowledge that our decoding results might be at least partially determined by the adoption
577 of a non-visually-guided memory-based task (see also Fabbri et al. 2010, 2012; Ariani et al. 2015,
578 2018; Leo et al. 2016; Turella et al. 2016). Our task imposed specific constraints during movement
579 execution which are different from requirements of classical open-loop paradigms - where the target
580 object is directly visible during planning, but not during execution - adopted in monkey (e.g. Fattori
581 et al. 2010) and human studies (e.g. Gallivan, McLean, Flanagan, et al. 2013). Nevertheless, even
582 considering the uncommon requirements of our paradigm, most of the reported findings,
583 particularly effector-independent encoding (level 3), are in line with previous investigations in the
584 field adopting a classical open-loop paradigm (Gallivan, McLean, Flanagan, et al. 2013).

585 In the following sections, we will focus on each specific cortical network to highlight its
586 properties, providing an overview of the implications of our findings for understanding the brain
587 architecture underlying hand-object interactions.

588

589 **Action encoding in frontal regions**

590 M1 has been classically considered as the final stage of the parieto-frontal system with the
591 crucial role of producing motor output. Therefore, the description of concrete action encoding in
592 this area is not surprising and is causally linked to perform an appropriate action. However, we also
593 obtained a wrist-independent, effector-specific goal representation in M1.

594 The representation of abstract information within M1 appears to be in line with recent fMRI
595 studies (Kadmon Harpaz et al. 2014; Leo et al. 2016). As an example, Kadman Harpaz (2014)
596 reported that M1 and aIPS encoded the movement of writing a specific letter with the dominant
597 hand independently of the size of the drawing within M1 and aIPS, suggesting a similarity of
598 encoding within these two regions. These findings confirmed that M1 entailed the functional
599 specificity needed to perform actions characterized by specific motor features but showed that, even
600 at the latest cortical stage of the motor system, there is also information about a more abstract goal -
601 even if only at an effector-dependent level (see also Kakei et al. 1999).

602 Likewise, Leo et al. (2016) showed that M1 represented hand movement information in terms
603 of synergies, i.e. meaningful patterns of joint movements/postures, measured with kinematic
604 recordings. This finding provided support for the idea that M1 does not only represent concrete
605 aspects of actions, but also more abstract information, as demonstrated in our study. Moreover,
606 brain activity was predictable on the basis of kinematic synergies not only within left M1 (Leo et al.
607 2016), but also within other regions of the hand motor network, such as contralateral premotor,
608 somatosensory, superior and inferior parietal regions, together with bilateral PMv and aIPS.
609 Relevant for our study, the authors showed similar synergy-based encoding for the dominant hand
610 not only within the left M1, but also within bilateral aIPS.

611 These two studies suggest possible similarities between the abstract representation within aIPS
612 and M1. Our study also revealed differences between these two regions. We obtained a functional
613 specialization within contralateral M1, where actions can be represented in flexible terms with
614 respect to their goal (i.e., irrespective of wrist orientation), but only at an effector-dependent level.
615 The parietal lobe contained similar effector-dependent encoding, but crucially hosting sites of

616 convergence within aIPS (and possibly left pIPS), which represented action goals at both an
617 effector-dependent and -independent level (see also Gallivan et al., 2013b, 2013c).

618

619 **Action encoding in parietal regions**

620 The PPC has been classically reported to be crucial for planning effector-specific actions
621 comprising specific modules for reaching, saccadic eye movements and grasping (Andersen and
622 Buneo 2002; Cui and Andersen 2007; Andersen et al. 2014). Our description of concrete action
623 encoding in the PPC perfectly supports this line of research.

624 Recent findings seem to complement our understanding of effector-specificity within the PPC by
625 investigating actions performed with multiple effectors, such as the eyes, the right hand and the
626 right foot (Heed et al. 2011, 2016; Leoné et al. 2014). In these studies, PPC regions do not seem to
627 follow only a strict effector-related organization, but could be involved in processing the same type
628 of action information (or function) regardless of the adopted effector (Heed et al. 2011). Moreover,
629 PPC might more likely represent dichotomies of effectors rather than a single specific one (Leoné et
630 al. 2014), so that effector specificity within PPC might be relative and not absolute in nature. This
631 representational organization within PPC could provide the possible neural mechanism for
632 representing an action goal both in terms of the selected effector (e.g. right hand) and of its potential
633 alternatives (e.g. right foot and/or eyes). Similarly, our analyses revealed PPC regions (aIPS, left
634 pIPS), where information about the same action goal is encoded jointly for the contra- and
635 ipsilateral hand, and irrespective of which hand will be adopted (see also Gallivan et al., 2013b).
636 Our conjunction results thus extend previous findings (Leoné et al. 2014) to grasping actions
637 performed with the same effector, but considering the two body sides (left vs right).

638 One might argue that a complementary interpretation of our data could be that these
639 representations are crucial for action and effector selection, providing a cohort of potential
640 movements - characterized by different motor features, such as effector, hand orientation and grip
641 type - among which to select the best candidate to-be-executed. This interpretation is in line with
642 the possible pivotal role of PPC in representing this possible landscape of motor options, emerging
643 from computational models of action selection (Cisek 2006) and empirical data on effector selection
644 (Oliveira et al. 2010; Fitzpatrick et al. 2019). While this interpretation seems plausible, we wish to
645 remark that our data are equally compatible with alternative views according to which the PPC
646 represent abstract (categorical) *outcomes* of decisions (e.g. Freedman and Assad 2011), which are

647 then implemented by selecting the most appropriate motor features. Our experiment was not
648 designed to distinguish between these alternative accounts.

649 From a broader perspective, parietal cortices seem to accommodate a wider set of action
650 representations with respect to frontal regions. This description seemed to suggest a gradient from a
651 representation of actions less bound to the selected effector within parietal cortices to a
652 representation which is more linked to a specific effector and motor features within frontal regions.
653 A similar transition between hand-independent and hand-specific coding has been recently
654 described at the neural level in monkey - during grasp planning - while recording from anterior
655 intraparietal cortex, area AIP, and ventral premotor cortex, area F5 (Michaels and Scherberger
656 2018).

657 Overall, our results suggest that the level at which actions are encoded differ between frontal and
658 parietal regions. Local computations within PPC regions, such as aIPS, might flexibly remap the
659 same goal to a different effector when required by the task, as recently proposed by other authors
660 (Heed et al. 2011, 2016; Leoné et al. 2014). Considering the likely bidirectional flow of information
661 within parieto-frontal networks (Schaffelhofer and Scherberger 2016; Blohm et al. 2019), in this
662 specific situation, the implementation of the remapped motor output would be possible by
663 transferring this information to premotor cortices and then to M1, where only effector-dependent
664 goal information is present.

665

666 **Differences in action representations between posterior and anterior parietal cortices**

667 The crucial role of the aIPS in representing different types of grasping actions is commonly
668 accepted (Janssen and Scherberger 2015). Lesions within the anterior part of the intraparietal cortex
669 led to an impairment in grasping both in monkeys (Gallese et al. 1994) and in humans (Binkofski et
670 al. 1998). Our findings provide an important extension of previous results on effector-independent
671 encoding (Gallivan, McLean, Flanagan, et al. 2013), demonstrating that this area serves as a
672 convergence for representations of action goals within and across the two hands. In addition to
673 aIPS, we showed a similar convergence of all three investigated levels of representation also within
674 a more posterior region within the parietal cortex, the pIPS (and pSPL in the conjunction analysis).

675 The posterior part of the of the intraparietal cortex (and the pSPL) has been traditionally assumed
676 to be involved in reaching, representing the direction and/or the target spatial position of the
677 performed or planned movement (Andersen and Buneo 2002). However, recent investigations

678 demonstrated the involvement of this area also in grasping actions both in monkeys (Fattori et al.
679 2009, 2010, 2012; Breveglieri et al. 2018) and in humans (Gallivan, McLean, Smith, et al. 2011;
680 Gallivan, McLean, Flanagan, et al. 2013; Gallivan, McLean, Valyear, et al. 2013; Fabbri et al. 2014;
681 Tosoni et al. 2015).

682 Haar et al. (2017) showed that posterior parietal regions, comprising the SPL, encode the
683 direction of the performed movement. In addition, ipsilateral and contralateral movements were
684 represented similarly, according to an intrinsic coordinate system. Fronto-parietal regions seemed to
685 host a representation of movement direction based on equivalent joint angles, which is invariant of
686 the adopted effector (left or right hand). These findings might suggest an interpretation of our
687 results in pSPL, and possibly also in pIPS, based on direction of the movement and/or spatial
688 position of the target. Note that this interpretation is not compatible with the paradigm adopted in
689 our study, as the spatial position of the target object was the same for movements with the right and
690 the left hand. Moreover, the direction of the movement in intrinsic/joint coordinates was the same
691 for all the actions performed with the two hands. This characteristic of our task thus might point
692 towards an interpretation of our results in left pSPL and pIPS in terms of a representation of actions
693 goals across the two hands, in accordance with the role of these regions in coding also grasp-related
694 information. This representation of action goals might coexist with the encoding of direction in
695 intrinsic/joint coordinates described by Haar et al. (2017).

696 A recent study on tool use (Gallivan, McLean, Valyear, et al. 2013) suggested potentially
697 different roles of pIPS and aIPS in representing action goals. In this investigation, Gallivan et al
698 (2013) compared grasping and reaching performed either with the right hand or with a plier. pIPS
699 hosted overlapping representations of concrete actions performed with the hand and with the tool,
700 together with a representation of action goal invariant to the use of the hand or of a tool. aIPS
701 showed a different response pattern, as it also represented concrete actions for both effectors (hand
702 and plier) but showed no representation of shared goals across these two effectors.

703 A comprehensive interpretation of ours and other results (Gallivan, McLean, Flanagan, et al.
704 2013; Gallivan, McLean, Valyear, et al. 2013; Haar et al. 2017) might suggest a representation of
705 action goals within and across hands – but not generalizing to tool action goals - within the anterior
706 part of PPC, whereas the posterior part of PPC might host a representation of actions goals together
707 with the encoding of the direction of the movement in a common effector-invariant code following
708 intrinsic coordinates. Different action- and position-related information would be stored in specific
709 pathways of the dorsal stream and might be differently recruited depending on task demands
710 (Galletti and Fattori 2018). Even if this is an intriguing proposal, it needs to be empirically tested by

711 employing a paradigm dissociating spatial position and action/goal encoding across hands and/or
712 tools.

713

714 **Action organization within temporal cortices**

715 Whereas our ROI analysis focused on parieto-frontal regions, the searchlight analysis revealed
716 decoding for different levels of action representations within temporal cortices (Figure 3A, Figures
717 S4-S9). Of particular interest for the present study is the specific organization of action encoding in
718 the left LOTC (Figure 3A). Within this region, we obtained significant decoding for the most
719 abstract level of goal encoding, but no overlap with the other levels of the hierarchy. Our
720 observations are in line with recent investigations showing goal encoding within the temporal lobe
721 during planning and execution (Gallivan, Chapman, et al. 2013; Ariani et al. 2015; Turella et al.
722 2016). We extended these results by showing a segregated organization, with an abstract (effector-
723 independent) representation of executed actions hosted within the LOTC. These results partly
724 mirror the organization described during action observation (Wurm and Lingnau 2015; Wurm et al.
725 2016), supporting the crucial role of the LOTC in representing abstract action information across a
726 range of stimuli and tasks (Lingnau and Downing 2015).

727 The LOTC might act as a site of integration for different types of information coming from the
728 dorsal and the ventral streams (Lingnau and Downing 2015), but the exact nature of the role of
729 these representations during tasks involving sensorimotor control is still poorly understood
730 (Gallivan and Culham 2015). Before an action is performed, specific sub-regions within the LOTC
731 and the dorsal stream might exchange information about the properties of the to-be-grasped object,
732 the planned action and/or of its expected sensory consequences (Gallivan and Culham 2015;
733 Zimmermann et al. 2016). During action execution, this information might be adopted for
734 monitoring and possible online corrections, but its exact contribution to motor control is difficult to
735 assess yet. A complementary interpretation might relate this significant decoding to motor imagery
736 of the planned or executed actions as participants could not see their own movements (Pilgramm et
737 al. 2016; Zabicki et al. 2017).

738 Further MVPA and connectivity studies will be needed to fully clarify the specific function of
739 the temporal cortex in motor control. Indeed, previous connectivity studies provided precious
740 information to constrain our interpretation of the present data (Grol et al. 2007; Verhagen et al.
741 2008; Hutchison and Gallivan 2018) and novel task-based connectivity approaches (Di and Biswal
742 2019) seem to be incredibly promising to further characterize the brain dynamics of the hand motor

743 network. Nevertheless, our description of abstract representational content has started to reveal the
744 complex structure of the neural organization of action representation hosted within the LOTC even
745 during motor execution.

746

747 **Conclusions**

748 Our results widened previous investigations on motor control, demonstrating that executed
749 actions are represented at different levels of abstraction following a hierarchical organization,
750 retaining a unique arrangement within frontal, parietal and temporal cortices. This neural
751 architecture is likely to underlie our ability to interact with the world, orchestrating the performance
752 of specific hand-object interactions. At the same time, this neural architecture might provide the
753 flexibility needed to react to unexpected changes in the environment, remapping an intended motor
754 goal, through the same effector - adopting another type of interaction with an object - or even
755 generating a different motor output - adopting another effector.

756 Finally, the description of these different levels of abstraction might be exploited for a possible
757 translational implementation of our work in the field of neuroprosthetics. Indeed, a confirmation of
758 the crucial role of the parietal cortex in representing “abstract” action goals emerged in a recent
759 neurophysiological investigation in humans (Aflalo et al. 2015). Here, a tetraplegic patient
760 controlled an external robotic hand by means of the neural signals recorded from anterior
761 intraparietal and superior parietal cortices (similar to the ones localized in our study). This finding
762 advised the adoption of MVPA of fMRI data as a precious guide to identify the most meaningful
763 cortical targets to implant multi-array electrodes for guiding brain machine interfaces.

764

765

Acknowledgements

This work was supported by the Provincia Autonoma di Trento and by the Fondazione Caritro. LT is supported by the “Futuro in Ricerca 2013” grant (FIRB 2013, project RBFR132BKP) awarded by MIUR. A.L. is supported by a German Research Foundation Heisenberg-Professorship Grant (Li 2840/2-1). The authors would like to thank Dr. Paolo Ferrari for technical support.

766

767 **References**

- 768 Aflalo T, Kellis S, Klaes C, Lee B, Shi Y, Pejsa K, Shanfield K, Hayes-Jackson S, Aisen M, Heck C, Liu C, Andersen
769 R. 2015. Decoding motor imagery from the posterior parietal cortex of a tetraplegic human. *Science* (80-).
770 348:906–910.
- 771 Andersen RA, Andersen KN, Hwang EJ, Hauschild M. 2014. Optic Ataxia: From Balint’s Syndrome to the Parietal
772 Reach Region. *Neuron*. 81:967–983.
- 773 Andersen RA, Buneo CA. 2002. Intentional maps in posterior parietal cortex. *Annu Rev Neurosci*. 25:189–220.
- 774 Ariani G, Oosterhof NN, Lingnau A. 2018. Time-resolved decoding of planned delayed and immediate prehension
775 movements. *Cortex*. 99:330–345.
- 776 Ariani G, Wurm MF, Lingnau A. 2015. Decoding Internally and Externally Driven Movement Plans. *J Neurosci*.
777 35:14160–14171.
- 778 Barany D, Della-Maggiore V, Viswanathan S, Cieslak M, Grafton ST. 2014. Feature interactions enable decoding of
779 sensorimotor transformations for goal-directed movement. *J Neurosci*. 34:6860–6873.
- 780 Benjamini Y, Hochberg Y. 1995. Controlling the False Discovery Rate: a Practical and Powerful Approach to Multiple
781 Testing. *J R Stat Soc*. 57:289–300.
- 782 Beurze SM, de Lange FP, Toni I, Medendorp WP. 2007. Integration of target and effector information in the human
783 brain during reach planning. *J Neurophysiol*. 97:188–199.
- 784 Binkofski F, Dohle C, Posse S, Stephan KM, Hefter H, Seitz RJ, Freund HJ. 1998. Human anterior intraparietal area
785 subserves prehension: A combined lesion and functional MRI activation study. *Neurology*. 50:1253–1259.
- 786 Blohm G, Alikhanian H, Gaetz W, Goltz HC, DeSouza JFX, Cheyne DO, Crawford JD. 2019. Neuromagnetic
787 signatures of the spatiotemporal transformation for manual pointing. *Neuroimage*. 197:306–319.
- 788 Breveglieri R, Bosco A, Galletti C, Passarelli L, Fattori P. 2016. Neural activity in the medial parietal area V6A while
789 grasping with or without visual feedback. *Sci Rep*. 6:28893.
- 790 Breveglieri R, De Vitis M, Bosco A, Galletti C, Fattori P. 2018. Interplay Between Grip and Vision in the Monkey
791 Medial Parietal Lobe. *Cereb Cortex*. 28:2028–2042.
- 792 Chang SWC, Dickinson AR, Snyder LH. 2008. Limb-specific representation for reaching in the posterior parietal
793 cortex. *J Neurosci*. 28:6128–6140.
- 794 Chang SWC, Snyder LH. 2012. The representations of reach endpoints in posterior parietal cortex depend on which
795 hand does the reaching. *J Neurophysiol*. 107:2352–2365.
- 796 Cisek P. 2006. Integrated Neural Processes for Defining Potential Actions and Deciding between Them: A
797 Computational Model. *J Neurosci*. 26:9761–9770.
- 798 Cui H, Andersen RA. 2007. Posterior Parietal Cortex Encodes Autonomously Selected Motor Plans. *Neuron*. 56:552–
799 559.
- 800 Culham JC, Cavina-Pratesi C, Singhal A. 2006. The role of parietal cortex in visuomotor control: what have we learned
801 from neuroimaging? *Neuropsychologia*. 44:2668–2684.
- 802 Culham JC, Valyear KF. 2006. Human parietal cortex in action. *Curr Opin Neurobiol*. 16:205–212.
- 803 Di X, Biswal BB. 2019. Toward Task Connectomics: Examining Whole-Brain Task Modulated Connectivity in
804 Different Task Domains. *Cereb Cortex*. 29:1572–1583.
- 805 Fabbri S, Caramazza A, Lingnau A. 2010. Tuning curves for movement direction in the human visuomotor system. *J*
806 *Neurosci*. 30:13488–13498.
- 807 Fabbri S, Caramazza A, Lingnau A. 2012. Distributed sensitivity for movement amplitude in directionally tuned
808 neuronal populations. *J Neurophysiol*. 107:1845–1856.
- 809 Fabbri S, Strnad L, Caramazza A, Lingnau A. 2014. Overlapping representations for grip type and reach direction.
810 *Neuroimage*. 94:138–146.
- 811 Fattori P, Breveglieri R, Bosco A, Gamberini M, Galletti C. 2017. Vision for Prehension in the Medial Parietal Cortex.
812 *Cereb Cortex*. 27:1149–1163.
- 813 Fattori P, Breveglieri R, Marzocchi N, Filippini D, Bosco A, Galletti C. 2009. Hand orientation during reach-to-grasp
814 movements modulates neuronal activity in the medial posterior parietal area V6A. *J Neurosci*. 29:1928–1936.
- 815 Fattori P, Breveglieri R, Raos V, Bosco a., Galletti C. 2012. Vision for Action in the Macaque Medial Posterior Parietal

816 Cortex. *J Neurosci.* 32:3221–3234.

817 Fattori P, Raos V, Breveglieri R, Bosco A, Marzocchi N, Galletti C. 2010. The dorsomedial pathway is not just for
818 reaching: grasping neurons in the medial parieto-occipital cortex of the macaque monkey. *J Neurosci.* 30:342–
819 349.

820 Filimon F. 2010. Human cortical control of hand movements: parietofrontal networks for reaching, grasping, and
821 pointing. *Neuroscientist.* 16:388–407.

822 Fitzpatrick AM, Dundon NM, Valyear KF. 2019. The neural basis of hand choice: An fMRI investigation of the
823 Posterior Parietal Interhemispheric Competition model. *Neuroimage.* 185:208–221.

824 Freedman DJ, Assad JA. 2011. A proposed common neural mechanism for categorization and perceptual decisions. In:
825 *Nature Neuroscience.*

826 Gallese V, Murata A, Kaseda M, Niki N, Sakata H. 1994. Deficit of hand preshaping after muscimol injection in
827 monkey parietal cortex. *Neuroreport.* 5:1525–1529.

828 Galletti C, Fattori P. 2018. The dorsal visual stream revisited: Stable circuits or dynamic pathways? *Cortex.* 98:203–
829 217.

830 Gallivan JP, Chapman CS, McLean DA, Flanagan JR, Culham JC. 2013. Activity patterns in the category-selective
831 occipitotemporal cortex predict upcoming motor actions. *Eur J Neurosci.* 38:2408–2424.

832 Gallivan JP, Culham JC. 2015. Neural coding within human brain areas involved in actions. *Curr Opin Neurobiol.*
833 33:141–149.

834 Gallivan JP, McLean DA, Flanagan JR, Culham JC. 2013. Where one hand meets the other: limb-specific and action-
835 dependent movement plans decoded from preparatory signals in single human frontoparietal brain areas. *J*
836 *Neurosci.* 33:1991–2008.

837 Gallivan JP, McLean DA, Smith FW, Culham JC. 2011. Decoding effector-dependent and effector-independent
838 movement intentions from human parieto-frontal brain activity. *J Neurosci.* 31:17149–17168.

839 Gallivan JP, McLean DA, Valyear KF, Culham JC. 2013. Decoding the neural mechanisms of human tool use. *Elife.*
840 2:e00425.

841 Gallivan JP, McLean DA, Valyear KF, Pettypiece CE, Culham JC. 2011. Decoding action intentions from preparatory
842 brain activity in human parieto-frontal networks. *J Neurosci.* 31:9599–9610.

843 Grafton ST. 2010. The cognitive neuroscience of prehension: recent developments. *Exp brain Res.* 204:475–491.

844 Grol MJ, Majdandzic J, Stephan KE, Verhagen L, Dijkerman HC, Bekkering H, Verstraten FAJ, Toni I. 2007. Parieto-
845 Frontal Connectivity during Visually Guided Grasping. *J Neurosci.* 27:11877–11887.

846 Haar S, Dinstein I, Shelef I, Donchin O. 2017. Effector-Invariant Movement Encoding in the Human Motor System. *J*
847 *Neurosci.* 37:1663–17.

848 Haar S, Donchin O, Dinstein I. 2015. Dissociating Visual and Motor Directional Selectivity Using Visuomotor
849 Adaptation. *J Neurosci.* 35:6813–6821.

850 Heed T, Beurze SM, Toni I, Röder B, Medendorp WP. 2011. Functional rather than effector-specific organization of
851 human posterior parietal cortex. *J Neurosci.* 31:3066–3076.

852 Heed T, Leone FTM, Toni I, Medendorp WP. 2016. Functional versus effector-specific organization of the human
853 posterior parietal cortex: revisited. *J Neurophysiol.* 116:1885–1899.

854 Hutchison RM, Gallivan JP. 2018. Functional coupling between frontoparietal and occipitotemporal pathways during
855 action and perception. *Cortex.* 98:8–27.

856 Janssen P, Scherberger H. 2015. Visual Guidance in Control of Grasping. *Annu Rev Neurosci.* 38:150403170110009.

857 Kadmon Harpaz N, Flash T, Dinstein I. 2014. Scale-invariant movement encoding in the human motor system. *Neuron.*
858 81:452–461.

859 Kakei S, Hoffman DS, Strick PL. 1999. Muscle and movement representations in the primary motor cortex. *Science.*
860 285:2136–2139.

861 Karnath H-OO, Perenin M-TT. 2005. Cortical control of visually guided reaching: evidence from patients with optic
862 ataxia. *Cereb Cortex.* 15:1561–1569.

863 Krasovsky A, Gilron R, Yeshurun Y, Mukamel R. 2014. Differentiating intended sensory outcome from underlying
864 motor actions in the human brain. *J Neurosci.* 34:15446–15454.

865 Kriegeskorte N, Bandettini P. 2007. Combining the tools: activation- and information-based fMRI analysis.

866 Neuroimage. 38:666–668.

867 Leo A, Handjaras G, Bianchi M, Marino H, Gabiccini M, Guidi A, Scilingo EP, Pietrini P, Bicchi A, Santello M,
868 Ricciardi E. 2016. A synergy-based hand control is encoded in human motor cortical areas. *Elife*. 5:1–32.

869 Leoné FTM, Heed T, Toni I, Medendorp WP. 2014. Understanding effector selectivity in human posterior parietal
870 cortex by combining information patterns and activation measures. *J Neurosci*. 34:7102–7112.

871 Lingnau A, Downing PE. 2015. The lateral occipitotemporal cortex in action. *Trends Cogn Sci*. 19:268–277.

872 Michaels JA, Scherberger H. 2018. Population coding of grasp and laterality-related information in the macaque fronto-
873 parietal network. *Sci Rep*. 8:1710.

874 Nelissen K, Fiave PA, Vanduffel W. 2017. Decoding Grasping Movements from the Parieto-Frontal Reaching Circuit
875 in the Nonhuman Primate. *Cereb Cortex*. 465:1–15.

876 Nichols T, Brett M, Andersson J, Wager T, Poline JB. 2005. Valid conjunction inference with the minimum statistic.
877 *Neuroimage*. 25:653–660.

878 Oliveira FTP, Diedrichsen J, Verstynen T, Duque J, Ivry RB. 2010. Transcranial magnetic stimulation of posterior
879 parietal cortex affects decisions of hand choice. *Proc Natl Acad Sci U S A*. 107:17751–17756.

880 Oosterhof NN, Connolly AC, Haxby J V. 2016. CoSMoMMPA: Multi-Modal Multivariate Pattern Analysis of
881 Neuroimaging Data in Matlab/GNU Octave. *Front Neuroinform*. 10:27.

882 Oosterhof NN, Tipper SP, Downing PE. 2012a. Visuo-motor imagery of specific manual actions: a multi-variate pattern
883 analysis fMRI study. *Neuroimage*. 63:262–271.

884 Oosterhof NN, Tipper SP, Downing PE. 2012b. Viewpoint (in)dependence of action representations: an MVPA study. *J
885 Cogn Neurosci*. 24:975–989.

886 Oosterhof NN, Wiestler T, Downing PE, Diedrichsen J. 2011. A comparison of volume-based and surface-based multi-
887 voxel pattern analysis. *Neuroimage*. 56:593–600.

888 Pilgramm S, de Haas B, Helm F, Zentgraf K, Stark R, Munzert J, Krüger B. 2016. Motor imagery of hand actions:
889 Decoding the content of motor imagery from brain activity in frontal and parietal motor areas. *Hum Brain Mapp*.
890 37:81–93.

891 Rizzolatti G, Camarda R, Fogassi L, Gentilucci M, Luppino G, Matelli M. 1988. Functional organization of inferior
892 area 6 in the macaque monkey. *Exp Brain Res*. 71:491–507.

893 Rizzolatti G, Cattaneo L, Fabbri-Destro M, Rozzi S. 2014. Cortical mechanisms underlying the organization of goal-
894 directed actions and mirror neuron-based action understanding. *Physiol Rev*. 94:655–706.

895 Rizzolatti G, Luppino G, Matelli M. 1998. The organization of the cortical motor system: new concepts.
896 *Electroencephalogr Clin Neurophysiol*. 106:283–296.

897 Schaffelhofer S, Scherberger H. 2016. Object vision to hand action in macaque parietal, premotor, and motor cortices.
898 *Elife*. 5:1–24.

899 Smith SM, Nichols TE. 2009. Threshold-free cluster enhancement: Addressing problems of smoothing, threshold
900 dependence and localisation in cluster inference. *Neuroimage*. 44:83–98.

901 Tosoni A, Pitzalis S, Committeri G, Fattori P, Galletti C, Galati G. 2015. Resting-state connectivity and functional
902 specialization in human medial parieto-occipital cortex. *Brain Struct Funct*. 220:3307–3321.

903 Tucciarelli R, Turella L, Oosterhof NN, Weisz N, Lingnau A. 2015. MEG Multivariate Analysis Reveals Early Abstract
904 Action Representations in the Lateral Occipitotemporal Cortex. *J Neurosci*. 35:16034–16045.

905 Turella L, Lingnau A. 2014. Neural correlates of grasping. *Front Hum Neurosci*. 8:686.

906 Turella L, Tucciarelli R, Oosterhof NNN, Weisz N, Rumiati R, Lingnau A. 2016. Beta band modulations underlie
907 action representations for movement planning. *Neuroimage*. 136:197–207.

908 Valyear KF, Frey SH. 2015. Human posterior parietal cortex mediates hand-specific planning. *Neuroimage*. 114:226–
909 238.

910 Verhagen L, Dijkerman HC, Grol MJ, Toni I. 2008. Perceptuo-Motor Interactions during Prehension Movements. *J
911 Neurosci*. 28:4726–4735.

912 Vesia M, Crawford JD. 2012. Specialization of reach function in human posterior parietal cortex. *Exp brain Res*. 221:1–
913 18.

914 Wurm MF, Ariani G, Greenlee MW, Lingnau A. 2016. Decoding Concrete and Abstract Action Representations During
915 Explicit and Implicit Conceptual Processing. *Cereb Cortex*. 26:3390–3401.

- 916 Wurm MF, Lingnau A. 2015. Decoding actions at different levels of abstraction. *J Neurosci.* 35:7727–7735.
- 917 Zabicki A, De Haas B, Zentgraf K, Stark R, Munzert J, Krüger B. 2017. Imagined and executed actions in the human
918 motor system: Testing neural similarity between execution and imagery of actions with a multivariate approach.
919 *Cereb Cortex.* 27:4523–4536.
- 920 Zaitsev M, Hennig J, Speck O. 2004. Point spread function mapping with parallel imaging techniques and high
921 acceleration factors: Fast, robust, and flexible method for echo-planar imaging distortion correction. *Magn Reson*
922 *Med.* 52:1156–1166.
- 923 Zimmermann M, Verhagen L, Lange FP De, Toni I. 2016. The Extrastriate Body Area Computes Desired Goal States
924 during Action Planning 1 , 2 , 3. 3:1–13.
- 925